A PRELIMINARY NUMERICAL EXPERIMENT IN SIMULATING THE DISPERSION OF SF_6

Fred J. Kopp
Institute of Atmospheric Sciences
South Dakota School of Mines and Technology
Rapid City, South Dakota 57701-3995

Abstract. A numerical simulation of an SF_6 tracer experiment conducted on July 19, 1985, in North Dakota has been made. Both SF_6 and AgI seeding are simulated in the model, although not concurrently. Only one seeding agent is simulated in a particular run of the model. The numerical experiments show that the SF_6 and AgI will disperse in a similar fashion initially but, as the AgI is activated inside the cloud, there will be some differences. The development of detectable ice and precipitation as a result of AgI seeding will likely diverge somewhat from the SF_6 dispersion.

1. INTRODUCTION

The efficacy of the dispersal of seeding materials in clouds that are to be treated has been under question for some time (Stith et al., 1986). Researchers have dispersed seeding materials into the updrafts below cloud base to minimize the possibility that the seeding materials are carried off away from the target clouds. This raises the question of how much the seeding material is dispersed while being carried through the cloud. If the seeding material remains in a small volume, the seeding effects will affect only a small portion of the cloud leaving the greater portion of the cloud untreated, which is not the desired result. The seeding material is not easy to detect. In the case of CO_2, the seeding material is found in the atmosphere, in large quantities naturally, so detection of CO_2 gas is not evidence of seeding material. Warburton and Maher (1985) collected rainfall and analyzed the water for silver. Most of the seeded days resulted in the detection of silver, but so did some of the non-seeded days. While the results suggest that the seeding material does get into the precipitation, the questions posed on the dispersion of the seeding material in the cloud are not answered.

Stith et al. (1986) report on using sulfur hexafluoride (SF_6) as a tracer. This gas is not found in the atmosphere naturally and can be detected in very small amounts (parts per trillion). The experiment releases the SF_6 tracer into the cloud in the same manner as AgI is released. An instrumented aircraft is then used to detect the SF_6, allowing the movement of the gas to be traced with time. These experiments are expected to answer some of the questions raised in the above discussion with the following assumptions. The expectation is that the AgI seeding material nuclei will behave in much the same way until activation of the AgI. Sulfur hexafluoride is not washed out by the water droplets in the cloud, so the gas will outlast the AgI. Consequently, detection of the movement of SF_6 will only mimic the movement of the AgI for a limited time.

Numerical model experiments are being conducted to test the extent to which the SF_6 will simulate the AgI transport. The model assumes that the two materials will be transported in the same way, but that the AgI will be an active seeding agent and will therefore interact with the cloud. Essentially, the SF_6 is an inactive AgI agent in the modeling. The simulation will show the extent to which the SF_6 and the AgI disassociate from each other. Also the location of the ice and precipitation particles relative to the two seeding agents will be simulated.

2. CLOUD MODEL

The model (Orville and Kopp, 1977) was modified to simulate the movement of SF_6 on a grid with 100 meter spacing. Essentially, the seeding field in the model was modified to behave like the silver iodide but with no interaction apart from being advected by the winds. This modification permitted SF_6 to be simulated in addition to AgI and CO_2. Only one seeding agent was allowed in any single simulation, so the combined effects of seeding with two agents was not possible. An assumption was made that the AgI seeding effects produce a very small dynamic effect. In this case, the dynamic effects were small.

Also, the AgI was not followed in the model after the AgI nuclei were simulated to become active. Following activation, the activated AgI was removed leaving inactivated AgI. In nature, of course, the AgI would be present in the cloud ice crystals formed by the activated AgI nuclei. The model does not distinguish between natural ice and "seeded" ice. In theory, one can distinguish between a natural ice crystal and one produced by AgI by examining the crystals for AgI. In practice, finding silver in seeded precipitation has been ambiguous (Warburton and Maher, 1985).

The two dimensionality of the model constrains the simulation of the three-dimensional problem. Certainly, the seeding materials were dispersed in three dimensions in the experiments, but this cannot be simulated in the model. Nonetheless, the two-dimensional results can give insights that may help interpret the observations.

3. INITIALIZATION OF MODEL

Several simulations were made with the aircraft sounding taken July 19, 1985, near

Dickinson. This sounding was very dry with a mixing ratio of 6-7 gm kg^{-1} of water vapor in the boundary layer. There was also a very strong inversion between 650 and 700 hPa. Little convective activity would be expected from the sounding even with convergence or orographic lifting. Some moisture may have been advected in at some level to have produced the observed clouds. In any case, the model was given a bubble of moisture to enhance cloud formation. None of these simulations produced a particularly satisfactory cloud, however, primarily because the cloud tops were too low. For the results presented here, the Dickinson sounding was used in modified form. This sounding was taken in the morning at 1000 MDT and, while even drier, the upper level inversion was weaker. In the lower levels, the dew points were modified by using a descending aircraft sounding. This increased the mixing ratio to 7 gm kg^{-1} rather than the 5 or so that the Dickinson sounding indicated. A heat and moisture bubble was added in the lower layers of the model. The temperature was highest near the surface, decreasing above while the moisture was greatest in the center such that the maximum mixing ratio was about 1 km above the surface. The bubble had a maximum temperature excess of 3°C at the bottom, and mixing ratio excess of 8 gm kg^{-1} at the center, and decreased outward. The total mixing ratio in the bubble was 15 gm kg^{-1} at one point with a larger area of 10 to 12 gm kg^{-1} which was supersaturated. This resulted in instant cloud formation with a low cloud base.

At 9 min in the simulation, seeding material was introduced. Two seeding simulations were run. First, SF_6 seeding was simulated. The SF_6 was released in the middle of the cloud at a rate of 16 gm km^{-1}. The release was at 3.8 km MSL in an updraft, and the in-cloud temperature was near 0°C. A flight trajectory perpendicular to the plane of the model was assumed, so the seeding material was initially distributed in a circle.

Silver iodide seeding was also simulated in the exact position as the SF_6 so the AgI would follow the same trajectory until the effects of the AgI seeding affected the airflow. The same seeding rate was also used, although this was probably lower than the rate actually used in the field experiment.

4. RESULTS OF THE SIMULATIONS

The initial cloud base was at 1 km AGL, or about 1.8 km MSL, due to the bubble of excess moisture used to start the model. Within 10 min, the cloud base rose to 2.8 km MSL (Fig. 1), still

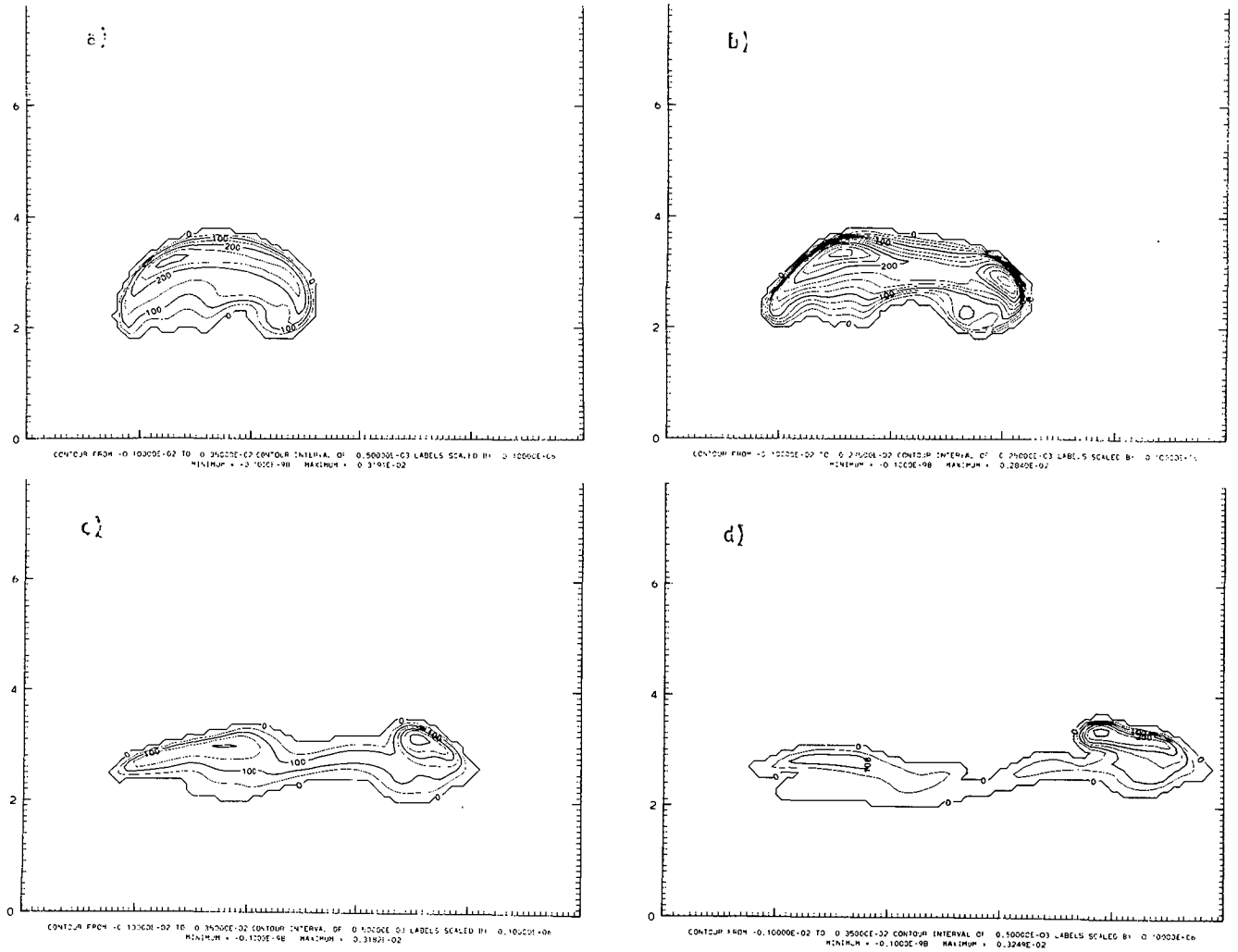

Fig. 1: Cloud water from SF_6 case but applicable to all cases: (a) At 9 min when seeding is done; (b) at 12 min. Note that the cloud is breaking apart. (c) 15 min; and (d) 18 min. In (c) and (d), the breakup of the cloud into two pieces is completed. Contours in gm gm^{-1}. See text for discussion.

somewhat lower than observed. The cloud base remained at approximately this level for the next few minutes. Cloud tops were about 4.8 km MSL, 9 min into the simulation and remained at this level for several minutes. By 18 min into the simulation, the cloud top fell to about 4.2 km MSL, and then fell gradually until the clouds dissipated at 34 min. The cloud on the right at 15 min (Fig. 1c) was formed by splitting away from the original cloud. Signs of the cloud splitting were evident at 12 min in Fig. 1b. As the initial thermal rose, the center cooled while the edges of the bubble retained a warm spot. A gravity wave formed and carried the right-hand part of the original cloud with it. The left-hand portion of the cloud probably was a gravity wave moving upstream that was held in place by the mean flow. The vertical motions at 12 min were broken into two main updraft regions located under the two centers of maximum cloud water in Fig. 1b. A downdraft developed, reaching to the surface between the left and right updrafts. This downdraft extended through the central part of the cloud in Fig. 1c and was responsible for the descending cloud top. By 18 min (Fig. 1d), the cloud was in essentially two parts, the split effectively completed by the downdraft.

4.1 Sulphur Hexafluoride Case

The SF_6 case was identical to the non-treated case, except that SF_6 was traced. Initially, the SF_6 cloud of gas was about 0.5 km per side with the core about half that size (Fig. 2a). After 3 min, the core concentration dropped by an order of magnitude and the cloud of gas had spread out into an elliptical shape 2 km wide by 1 km deep (Fig. 2). The expansion in the area covered was consistent with the decrease in maximum mixing ratio. As shown in Fig. 3, the concentration of SF_6 decayed exponentially with time. Also shown in Fig. 3 are the observed SF_6 concentrations for this case. The observations are trending downward also. In the first minute, the decrease was very sharp due to numerical spreading as the initial concentration was confined to a few grid points. The total mass of SF_6 remained constant in the grid within a few tenths of a percent so that the decrease in the maximum concentration was a result of an increase in the size of the SF_6 cloud (Fig. 2). Initially, the central maximum was carried upward and downwind. After 3 min, little of the SF_6 was left in the initial position and very little, if any, was transported upwind, as shown by the contours. Any upwind transport would have been due to diffusion. Six minutes after seeding, the center of the SF_6 cloud was lower than the initial cloud, although the top of the SF_6 extended as high as the original release. The SF_6 was being transported downward and to the right with the winds. No traces greater than 2 ppt of SF_6 were left at the initial release point. The cloud of tracer gas remained in a single cloud and was not split in two. In the next few minutes, the SF_6 continued to move with the airflow which carried the gas downward and downwind. At 21 and 24 min, the contour interval changed as the concentration of the SF_6 decreased to a few ppt so the enlargement of the gas cloud was somewhat exaggerated. The 200 contour at 21 and 24 min compares with the 25 contour (not labeled) at 18 min because the scaling on the labels changed by an order of magnitude. At 18 min (and before), the 50 contour label was 5 ppt, while in the last two plots, 200 was 2 ppt.

In the simulated time period from 15 to 21 min, the SF_6 gas cloud moved out of the water cloud that was seeded. The water cloud was dissipating, particularly in the downdraft, but the cloud's position was somewhat stationary, anchored to the initial updraft region where the bubble was introduced. After 18 min, the cloud dissipates and moves with the airflow.

4.2 Silver Iodide Case

The initial distribution of AgI was identical to the SF_6. This was done to make the comparison as easy as possible. The AgI was not conserved since it was active and interacted with the cloud microphysical process to produce ice crystals. Three minutes after seeding (Fig. 4a), there was a big difference between the SF_6 cloud and the AgI smoke cloud. Their positions were very similar, but the top of the AgI cloud appeared to be cut off with the contours becoming closely packed. The maximum mixing ratio was nearly an order of magnitude less than the SF_6 at this time. The freezing level was at the top of the AgI cloud, so the missing AgI was activated in the below freezing environment and was removed from the seeding agent field. Cloud ice (Fig. 5a) was growing at this time above the AgI cloud. At 15 min in the simulation, the AgI was more evenly dispersed, but the SF_6 extended to higher levels in the cloud. The AgI was carried by the airflow in much the same way as the SF_6. Compared at 18 and 21 min, the SF_6 and AgI fields continued to show similar patterns, with the basic difference, the expected absence of the AgI at below freezing temperatures.

Cloud ice (Fig. 5) appeared in the upper region of the seeded area of the cloud where the AgI field contours were cut off at 12 min. The cloud ice does not extend as high as the SF_6, the growth being concentrated near the initial AgI seeding location. The snow field (Fig. 6) was growing in the region of the cloud ice at 12 min and above. Much of the cloud ice appears to have been swept out in the uppermost regions by the snow, which was more extensive than the cloud ice at 12 min. At 15 min, the cloud ice field had two distinct growth areas, one in each cloud. The SF_6 and AgI contours (Figs. 2c and 4b) show that the AgI would have seeded them both. The snow was carried along with the the airflow as the SF_6 was, but at 15 min, the snow field was lagging behind the SF_6. This was also the case at 18 min, where the snow field was beginning to show unmistakable signs of melting when falling through the freezing level. The tightly packed contours were an indication of a sink in the production of snow. Figure 7 showed that the rain was forming from melted snow at 12 min as the snow field fell or was carried below the freezing level. The rain envelope followed the SF_6 outline in the lower levels until about 21 min when the rain began to fall below the level of SF_6.

5. CONCLUSIONS

The SF_6 and AgI did follow the same trajectories after release in the model. This was to be expected in the model since both substances are treated the same numerically. There were differences in the spread of the two fields, however. The differences were due to the AgI nuclei activating and forming ice crystals. Activated AgI

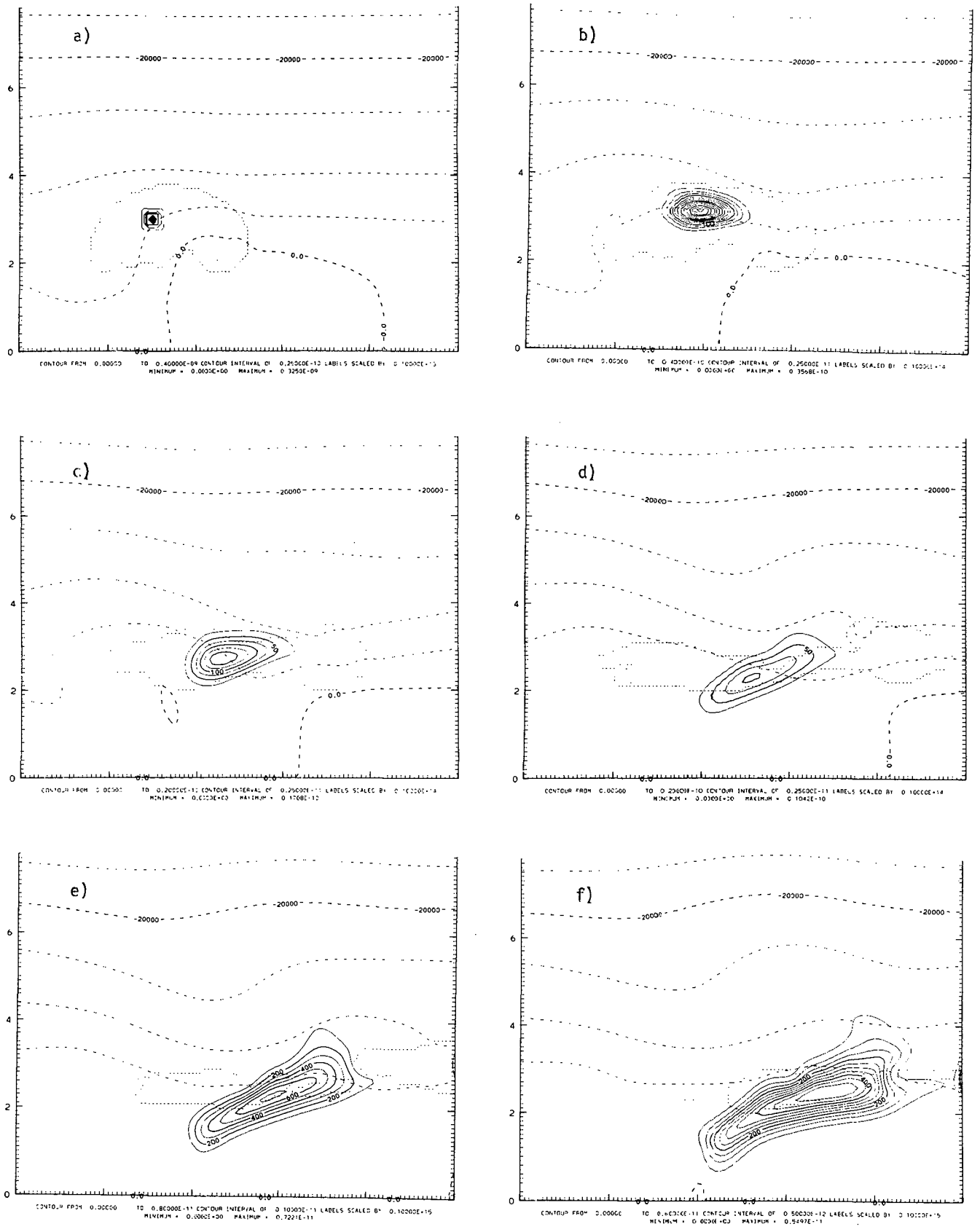

Fig. 2: Sulfur hexafluoride contours at (a) 9 min, through (f) at 24 min, with 3-min intervals. The initial distribution of SF_6 is shown in (a). In (b) through (d), the contour interval is constant at 2.5 ppt mixing ratio, changing in (e) to 1; and (f) to 0.5. The airflow carries the SF_6 along, spreading it out. See text for discussion.

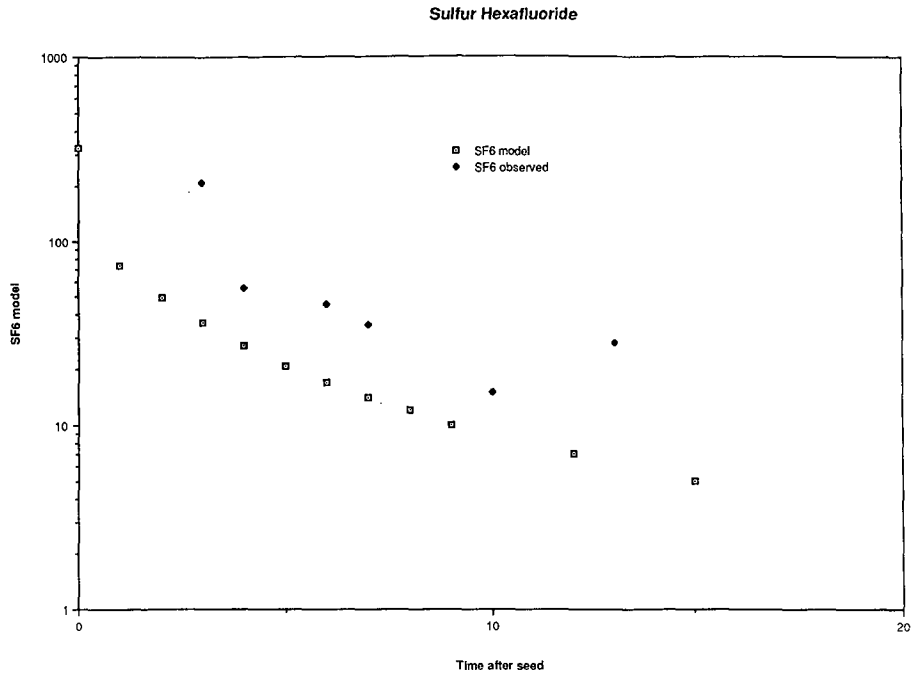

Fig. 3: Sulfur hexafluoride decay with time. The y-axis shows the maximum mixing ratio in gm per trillion gm of air. Time, on the x-axis, is in minutes from the beginning of the simulation. The results from the modeling are shown along with the observations made.

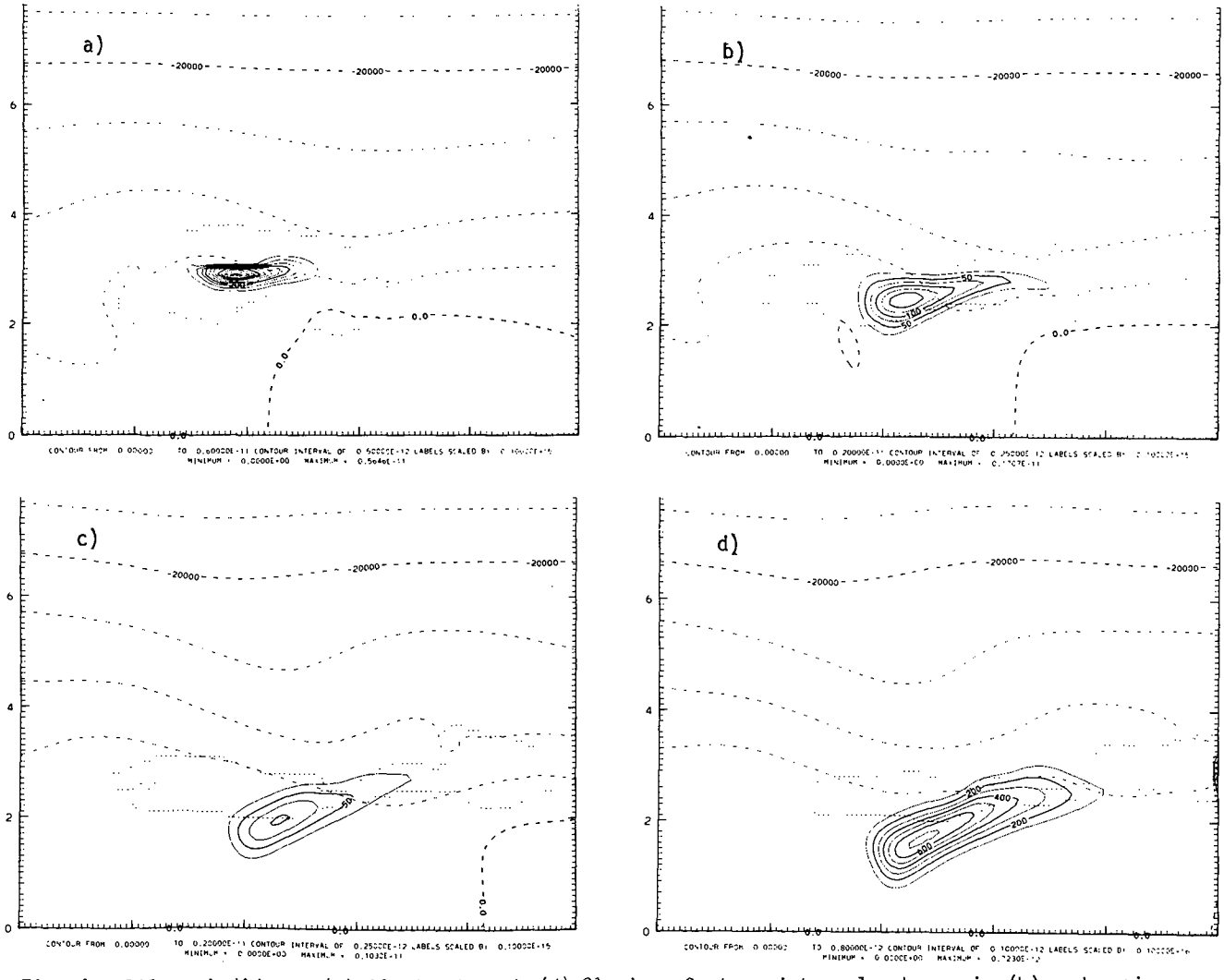

Fig. 4: Silver iodide at (a) 12 min through (d) 21 min. Contour intervals change in (b) and again in (d).

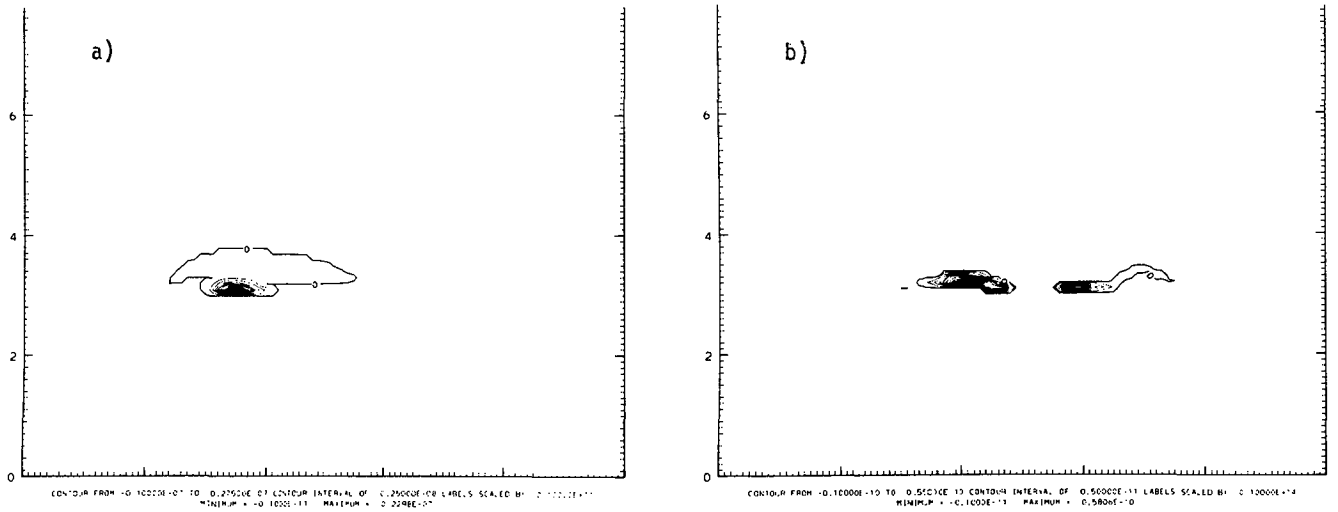

Fig. 5: Cloud ice in silver iodide case at 3-min intervals from 12 min in (a) to 15 min in (b). The mixing ratio is very small with the contour interval in (a) 2.5 ppb and 5 ppt in (b).

nuclei were removed from the AgI seeding field since they were no longer available for seeding.

One important result was that the precipitation can be displaced from the seeding field, as shown in Figs. 4b and 6b. Even though the snow was being carried along, there was growth in the snow contents. As the SF_6 was carried along, however, there was no growth. Consequently, the SF_6 tends to decay as it spreads while the snow grows. This displacement was not large and, in general, the precipitation seems to develop in the downwind half of the SF_6 field. The implications of this would be that SF_6 could be sampled while the expected precipitation particles may not be there, or that the precipitation might be detected while the SF_6 could be below the threshold for detection.

The other important result was that the concentration, as predicted by the model, indicated that the concentration of SF_6 falls off rapidly after release and would be one to two orders of magnitude less than the initial concentration as measured by detectors a few seconds after release.

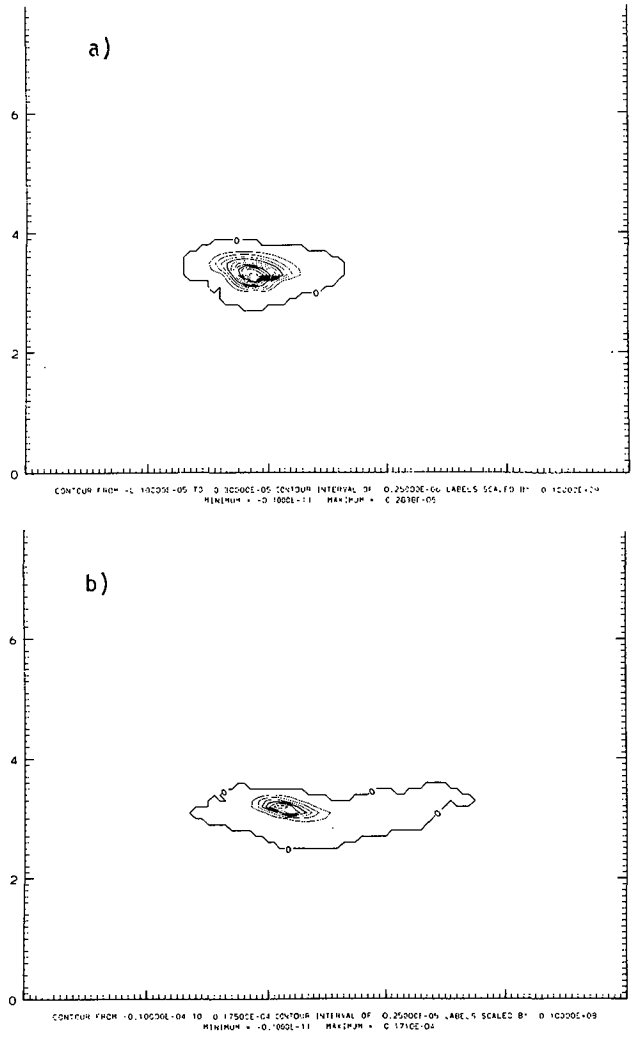

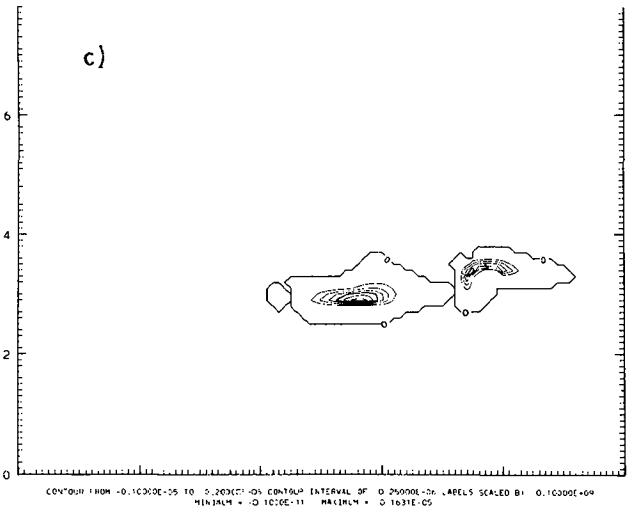

Fig. 6: Snow field from silver iodide case shown at (a) 12 min through (c) 18 min. The mixing ratio maximum and minimum are given in gm per gm air. The largest is a few hundredths of a gm kg^{-1}.

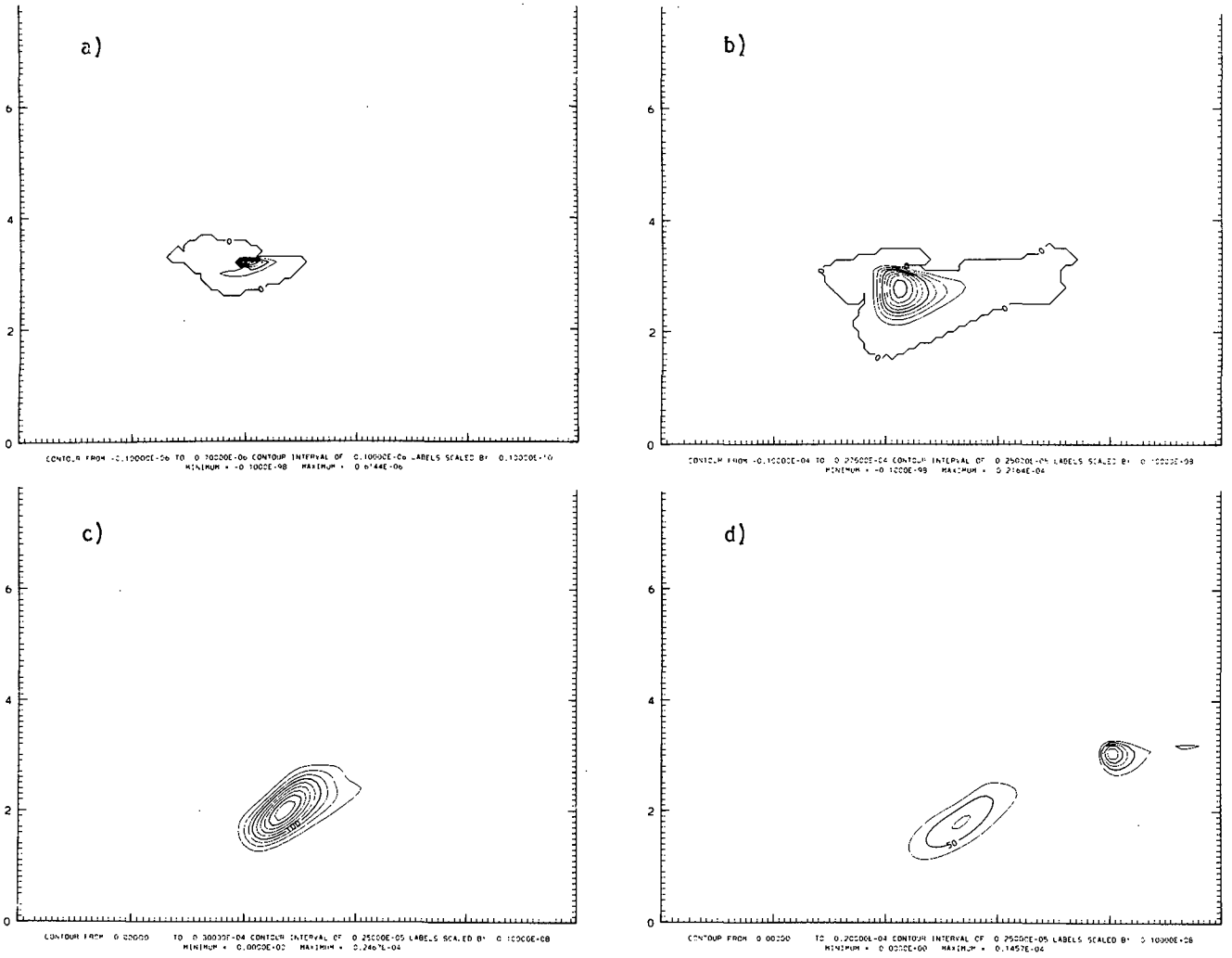

Fig. 7: Rainwater in the silver iodide case from (a) 12 min to (d) 21 min. The mixing ratio maximum and minimum are given in gm per gm air. They are very small, being a few hundredths of a gm kg^{-1}.

Observations (Stith et al., 1986) confirm these results. The observations tended to give a higher concentration, suggesting that the model may have too much diffusion or the initial conditions may have been different.

Acknowledgments. This work was supported by the North Dakota Atmospheric Resource Board under Contract No. ARB-IAS-87-1 and the National Science Foundation under Grant No. ATM-8516940. The computer simulations were done at the computing facilities of the Scientific Computing Division of the National Center for Atmospheric Research sponsored by the National Science Foundation.

Thanks also go to Mrs. Joie Robinson for preparation of the manuscript.

6. REFERENCES

Orville, H. D., and F. J. Kopp, 1977. Numerical simulation of the life history of a hailstorm. J. Atmos. Sci. 34:1596-1618. [Reply: J. Atmos. Sci., 35:10 (1978), 1554-1555.]

Stith, J. L., D. A. Griffith, R. L. Rose, J. Flueck, J. R. Miller and P. L. Smith, 1986. Aircraft observations of transport and diffusion in cumulus clouds. J. Climate Appl. Meteor., 25:1959-1970.

Warburton, J. A., and C. T. Maher, 1985. The detection of silver in rainwater: analysis of precipitation collected from cloud-seeding experiments. J. Climate Appl. Meteor. 4:560-564.